Effective Unconstrained Face Recognition by Combining Multiple Descriptors and Learned Background Statistics

Lior Wolf, *Member, IEEE,* Tal Hassner, and Yaniv Taigman

Abstract—Computer Vision and Biometrics systems have demonstrated considerable improvement in recognizing and verifying faces in digital images. Still, recognizing faces appearing in unconstrained, natural conditions remains a challenging task. In this paper we present a face-image, pair-matching approach primarily developed and tested on the "Labeled Faces in the Wild" (LFW) benchmark that reflect the challenges of face recognition from unconstrained images. The approach we propose makes the following contributions. (a) We present a family of novel face-image descriptors designed to capture statistics of local patch similarities. (b) We demonstrate how semi-labeled *background samples* may be used to better evaluate image similarities. To this end we describe a number of novel, effective similarity measures. (c) We show how labeled background samples, when available, may further improve classification performance, by employing a unique pair-matching pipeline. We present state-of-the-art results on the LFW pair-matching benchmarks. In addition, we show our system to be well suited for multi-label face classification (recognition) problems. We perform recognition tests on LFW images as well images from the laboratory controlled multiPIE database.

Index Terms—I.5.4.d Face and gesture recognition, I.5.3.b Similarity measures, Face recognition, Image descriptors, Similarity measures.

1 Introduction

Recent years have seen an explosion of visual media available through the Internet. This mounting volume of images and videos brings with it new opportunities and new challenges for Computer Vision applications. Face recognition applications in particular are now, more than ever, required to handle large quantities of images and remain accurate even when presented with images taken under unconstrained conditions. Facebook and Picasa web photo albums, for example, typically contain thousands of face images, most of which were obtained without control over facial expression, viewing angle, lighting conditions, occlusions and image quality. Such image collections strongly motivate research into recognition of faces in unconstrained images and at the same time provide an abundance of data for testing and developing new recognition techniques.

New recognition benchmarks have recently been published to facilitate the development of methods for face recognition under such challenging conditions. These include the "Labeled Faces in the Wild" (LFW) image set and benchmark [5], and the "Public Figures" (PubFig) data set of [6]. Both data sets consist of face images automatically harvested from news websites of known (labeled) people. The images in these sets thus attempt to capture the variability typical to unconstrained, "in the wild", face recognition problems. The LFW dataset in particular is published with a specific benchmark, which focuses on the face recognition task of *pair matching* (also referred to as "face verification"). In this task, given two face images, the goal is to decide whether the two pictures are of the same individual. Since its publication, the LFW benchmark has attracted quite a lot of attention, with various research teams contributing state-of-the-art pair-matching results [7].

This paper describes face pair-matching and classification methods developed and tested on the LFW benchmark and motivated by the following two principles. The first is that multiple image descriptors may be combined, each one complementing the others and together providing improved classification results. To this end we describe a family of novel descriptors which we show to be particularly useful for face recognition. The second principle is that face recognition performance (and indeed, classification performance in general) may greatly benefit from the availability of labeled *background* information. Here we refer to background samples as labeled training samples that do not belong to the classes being learned.

Our contributions in this paper are therefore the following:

1) We develop a family of novel image descriptors that are able to improve classification performance of multi-option recognition as well as pair-matching of face images. These descriptors

- *Parts of this manuscript have been published in [1]–[4].*
- *L. Wolf is with the School of Computer Science, Tel-Aviv University, Israel. E-mail: wolf@cs.tau.ac.il*
- *T. Hassner is with the Computer Science Division, The Open University of Israel. E-mail: hassner@openu.ac.il*
- *Y. Taigman is with face.com and with the School of Computer Science, Tel-Aviv University, Israel. E-mail: yaniv@face.com*

compute an image representation from local patch statistics. Here, we show these descriptors to provide information which is complementary to existing feature methods (see section 3).

2) We present two novel similarity measures, the One-Shot and the Two-Shot Similarity measures, both based on discriminative learning and both employing semi-labeled, background samples (section 4).
3) Finally, we show how labeled background samples may also be exploited to obtain more accurate classification results (section 4.4).

2 Existing methods

This paper touches on a number of well established research fields. We briefly survey relevant existing work.

Face recognition Face recognition is one of the most well-studied problems in Computer Vision and Biometrics and the literature on this problem is vast. Over the years a number of successful face-image data-sets have been published in an effort to facilitate research on face recognition. These include the Facial Recognition Technology (FERET) Database [8], the Face Recognition Grand Challenge (FRGC) facial images and depths along with accompanying benchmark tests [9], [10] and its successor, the Face Recognition Vendor Test (FRVT) database and benchmark [11], the CMU Pose Illumination and Expression (CMU-PIE) database [12] and its extension, the multi-PIE database [13].

These image sets were all designed to capture different sources of variability likely to be encountered by face recognition systems. These include illumination, pose, expression and more. However, they were all produced in controlled, laboratory settings. To provide researchers with a wider and more arbitrary range of viewing conditions, the Labeled Faces in the Wild (LFW) [5] and its extension, the Public Figure (PubFig) [6] sets were devised. These image sets include images automatically collected from Internet web pages; images were added to these sets if they include a face detected by a Viola and Jones face detector [14]. The facial images included in the LFW data set therefore demonstrate quite a bit of variability. Since its recent publication, a lot of attention has been focused on improving performance on the benchmarks associated with the LFW database (see, e.g., [1]–[3], [6], [15]–[19]).

Descriptor based methods for face recognition Face Images can be most readily described by statistics derived from their intensities. Intensities have thus served in many template-based methods. The intensities were sometimes normalized and sometimes replaced by edge responses [20]. More recently [21]–[23], Gabor wavelets have been used to describe the image appearance.

A texture descriptor called Local Binary Patterns (LBP) [24]–[26] has been shown to be extremely effective for face recognition [27]. The most simple form of LBP is created at a particular pixel location by threshholding the 3×3 neighborhood surrounding the pixel with the central pixel's intensity value, and treating the subsequent pattern of 8 bits as a binary number (Fig. 1). A histogram of these binary numbers in a predefined region is then used to encode the appearance of that region. The LBP representation of a given face image is generated by dividing the image into a grid of windows and computing histograms of the LBP values within each window. The concatenation of all these histograms constitutes the image's signature.

In this work we propose a patch-based descriptor that has some similarities to a variant of LBP called Center-Symmetric LBP (CSLBP) [28]. In CSLBP, eight intensities around a central point are measured. These intensities are spread evenly at a circle every 45 degrees starting at 12 o'clock. The binary vector encoding the local appearence at the central point, consists of four bits which contain the comparison of intensities to intensities on the symmetric position (180 degrees/ 6 hours difference).

Multi-block LBP [29] is an LBP variant that replaces intensity values in the computation of LBP with the mean intensity value of image blocks. Despite the similarity in terms, this method is very much different from our own. Multi-block LBP is shown to be effective for face detection, and in our initial set of experiments does not perform well for face recognition.

Modern image similarity learning techniques The literature on similarity functions is extensive. Some similarity measures proposed in the past have been hand crafted (e.g., [30], [31]). Alternatively, a growing number of authors have proposed tailoring similarity measures to available training data by applying learning techniques (e.g., [32]–[36]). In all these methods testing is performed using models (or similarity measures) learned beforehand.

The One-Shot and Two-Shot Similarity scores (OSS and TSS scores) introduced here (Section 4.1) are alternative approaches, designed to utilize "background" samples. OSS and TSS both draw their motivation from the growing number of so called "One-Shot Learning" techniques; that is, methods which learn from one or few training examples (see for example [37], [38]). Unlike previous methods for computing similarities, these novel similarity measures are computed by training a discriminative model *exclusive* to the two signals being compared, by using a set of background samples. As we will show, both measures are instrumental in obtaining state-of-the-art results on the Labeled Faces in the Wild (LFW) image pair-matching and provided boosted performance in multi-subject recognition problems.

Employing background samples differs from semi-supervised learning [39] and from transductive learning [40] since in both cases the unlabeled samples belong to the set of training classes. It differs from flavors of transfer learning that use unlabeled samples [41], since they use separate supervised learning tasks in order to benefit from the unlabeled set.

Although learning with background samples can be seen as belonging to the group of techniques called

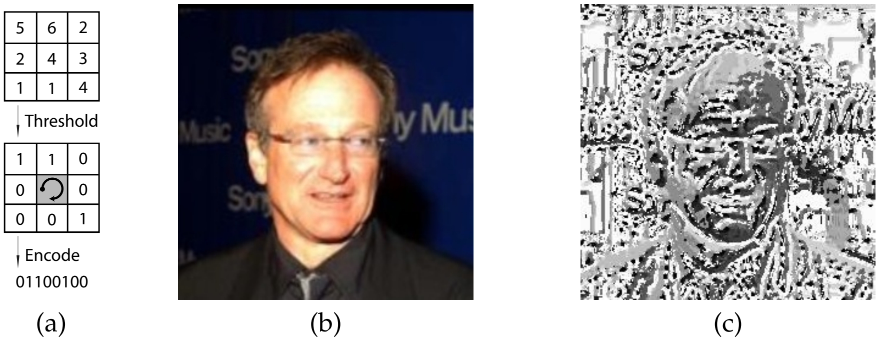

Fig. 1. (a) The LBP image-texture descriptor is computed locally at each pixel location. It considers a small neighborhood of a pixel, and thresholds all values by the central pixel's value. The bits which represent the comparison results are then transformed into a binary number. The histogram of these numbers is used as a signature describing the texture of the image. (b-c) Present an example image from the LFW data set, and its LBP encoding (different intensities representing different codes.)

"learning with side-information", it differs from existing methods in the literature known to us. In particular, some of the previous contributions, e.g., [36], [42], [43], require having training samples with the same identity. Other side-information contributions, e.g., [44] assume that the variability in the side information differs from that in the relevant data.

Also related to our work is the recent method of [6]. They study trait- or identity-based classifier-outputs as a feature for identification. Unlike our work, their method encodes one vector per face image whereas we encode pairs of images.

As a part of our supervised ("unrestricted") pipeline, we use a particular metric learning method called Information Theoretic Metric Learning (ITML) [45], [46]. ITML is a supervised metric learning technique for learning a Mahalanobis distance. It uses pairs of examples belonging to the same class (in our case, images of the same person) which are constrained to have similarities below a specified threshold. The similarities of pairs of points from different classes are constrained to have similarities above a second threshold. A regularization term ensures that the learned metric is similar to the original metric. The ITML method was shown to be extremely potent in Computer Vision problems [46]. The OSS and the TSS methods are both semi-supervised learning techniques. We show the OSS to work particularly well when combined with the supervised ITML method.

Patch-based approaches in recognition In this work we build upon methods which utilize image-patches, sometimes referred to as windows or blocks, for recognition. The patch based approach of [47] provides state of the art capabilities in similarity learning of faces and of general images. Other successful object recognition systems based on patches include the hierarchical system of [48].

The ability to detect local texture properties by examining the cross correlation between a central patch and nearby patches has been demonstrated in the texture segmentation system of [49]. In [50] a central patch was compared to surrounding patches to create a descriptor which extends the shape-context [30] descriptor to intensity images. The resulting descriptor has been shown to be highly invariant to image style and local appearance.

3 Novel patch based LBPs

The LBP descriptor and its variants (e.g., [29], [51]) use short binary strings to encode properties of the local micro-texture around each pixel. CSLBP [28], for example, encodes in each pixel the gradient signs at the pixel in four different angles. Here we propose two families of related descriptors, the Three-Patch LBP and the Four-Patch LBP descriptors[1], designed to encode additional types of local texture information.

The design of these descriptors is inspired by the Self-Similarity descriptor of [50]. Specifically, we explore ways of using short bit strings to encode similarities between neighboring patches of pixels in an effort to capture information complementary to that of pixel-based descriptors. Thus, employing patch based and pixel based descriptors in concert improves the overall accuracy of a classification system. In fact, a recent independent study [19] has shown that using our FPLBP descriptors described below to encode face images was only slightly worst than using collections of SIFT [52] descriptors, while being an order of magnitude more compact.

3.1 Three-Patch LBP Codes

Three-Patch LBP (TPLBP) codes are produced by comparing the values of three patches to produce a single bit value in the code assigned to each pixel. For each pixel in the image, we consider a $w \times w$ patch centered on the pixel, and S additional patches distributed uniformly in a ring of radius r around it (Fig. 2). For a parameter

[1] MATLAB code for computing both descriptors is available online at http://www.openu.ac.il/home/hassner/projects/Patchlbp/

α, we take pairs of patches, α-patches apart along the circle, and compare their values with those of the central patch. The value of a single bit is set according to which of the two patches is more similar to the central patch. The resulting code has S bits per pixel. Specifically, we produce the Three-Patch LBP by applying the following formula to each pixel:

$$\mathtt{TPLBP}_{r,S,w,\alpha}(p) = \sum_{i=1}^{S} f(d(C_i, C_p) - d(C_{i+\alpha \mod S}, C_p))2^i \tag{1}$$

Where C_i and $C_{i+\alpha \mod S}$ are two patches along the ring and C_p is the central patch. The function $d(\cdot,\cdot)$ is any distance function between two patches (e.g., L_2 norm of their gray level differences) and f is defined as:

$$f(x) = \begin{cases} 1 & \text{if } x \geq \tau \\ 0 & \text{if } x < \tau \end{cases} \tag{2}$$

We use a value τ slightly larger than zero (e.g., $\tau = 0.01$) to provide some stability in uniform regions, similarly to [28]. In practice, we use nearest neighbor sampling to obtain the patches instead of interpolating their values, as this speeds up processing with little or no effect on performance.

Once encoded, an image's signature is produced similarly to that of the CSLBP descriptor [28]. The image is divided into a grid of none-overlapping regions and a histogram measuring the frequency of each binary code is computed for each region. Each of these histograms are normalized to unit length, their values truncated at 0.2, and then once again normalized to unit length. An image is represented by these histograms concatenated to a single vector.

3.2 Four-Patch LBP Codes

For every pixel in the image, we look at two rings of radii r_1 and r_2 centered on the pixel, and S patches of size $w \times w$ spread out evenly on each ring (Fig. 3). To produce the Four-Patch LBP (FPLBP) codes we compare two center symmetric patches in the inner ring with two center symmetric patches in the outer ring positioned α patches away along the circle (say, clockwise). One bit in each pixel's code is set according to which of the two pairs being compared is more similar. Thus, for S patches along each circle we have $S/2$ center symmetric pairs which is the length of the binary codes produced. The resulting codes, similarly to the CS-LBP descriptors, are extremely compact, typically requiring histograms of only 16 values, yet have very high descriptive power, as was shown in [19].

The formal definition of the FPLBP code is as follows:

$$\begin{aligned}\mathtt{FPLBP}_{r_1,r_2,S,w,\alpha}(p) = \; & \sum_{i=1}^{S/2} f(d(C_{1i}, C_{2,i+\alpha \mod S}) - \\ & d(C_{1,i+S/2}, C_{2,i+S/2+\alpha \mod S}))2^i\end{aligned} \tag{3}$$

The final image signature is produced by using the same two-step normalization procedure described in Section 3.1.

4 Computing Similarity with Background Samples

In a learning framework, we define *background samples* as samples that do not belong to the classes being learned. Collecting such samples is often easy as they do not require labeling. In a face identification scenario these samples could be a face set of individuals not among those which the system is being trained to recognize. Besides being easy to collect, we believe such examples may provide valuable information about which images may be considered "the same" and which may not. In this section we present three novel similarity measures designed to exploit available background information for more accurate signal classification.

Why would background samples be useful for defining similarity functions? The sample vectors are embedded in a vector space in which various metrics can be employed. In order to know which metric is most suitable for the similarity task at hand, the underlying structure of the manifold on which the samples reside needs to be analyzed. Supervised learning can sometimes be used, but may require extra labeling information. On the other hand, background samples without additional information directly answer questions such as "is this sample closer to that one than to a typical example from the background set?" (the One-Shot Similarity, Section 4.1); "are these two examples well separated from the background sample set?" (the Two-shot Similarity, Section 4.1); and "do these two samples have similar sets of neighboring samples in the background set?" (ranking based similarity, Section 4.3).

4.1 The One-Shot and Two-Shot Similarity Measures

Given two vectors $\mathbf{I}$ and $\mathbf{J}$ their One-Shot Similarity (OSS) score is computed by considering a training set of background sample vectors $\mathbf{A}$. This set contains examples of items not belonging to the same class as neither $\mathbf{I}$ nor $\mathbf{J}$, but are otherwise unlabeled. A measure of the similarity of $\mathbf{I}$ and $\mathbf{J}$ is then obtained as follows (see also Fig. 4 (a)). First, a discriminative model is learned with $\mathbf{I}$ as a single positive example, and $\mathbf{A}$ as a set of negative examples. This model is then used to classify the vector, $\mathbf{J}$, and obtain a confidence score. The nature of this score depends on the classifier used. Using linear SVM, for example, this score may be the signed distance of $\mathbf{J}$ from the hyperplane separating $\mathbf{I}$ and $\mathbf{A}$. A second such score is then obtained by repeating the same process with the roles of $\mathbf{I}$ and $\mathbf{J}$ switched. The final OSS score is the average of these two scores.

The Two-Shot similarity (TSS) score is obtained in a single step by modifying the process described above (see also Fig. 4 (b)). Again, we consider the same auxiliary set of negative examples $\mathbf{A}$. This time, however,

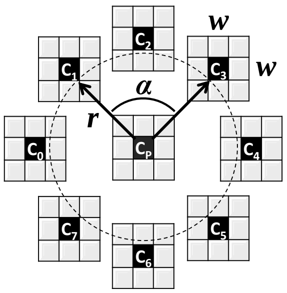

(a)

$$\begin{aligned}&\texttt{TPLBP}_{r,8,3,2}(p) =\\&f(d(C_0,C_p)-d(C_2,C_p))2^0+\\&f(d(C_1,C_p)-d(C_3,C_p))2^1+\\&f(d(C_2,C_p)-d(C_4,C_p))2^2+\\&f(d(C_3,C_p)-d(C_5,C_p))2^3+\\&f(d(C_4,C_p)-d(C_6,C_p))2^4+\\&f(d(C_5,C_p)-d(C_7,C_p))2^5+\\&f(d(C_6,C_p)-d(C_0,C_p))2^6+\\&f(d(C_7,C_p)-d(C_1,C_p))2^7\end{aligned}$$

(b)

(c)

Fig. 2. (a) The Three-Patch LBP code with $\alpha = 2$ and $S = 8$. (b) The TPLBP code computed with parameters $S = 8$, $w = 3$, and $\alpha = 2$. (c) Code image produced from the image in Fig. 1(b).

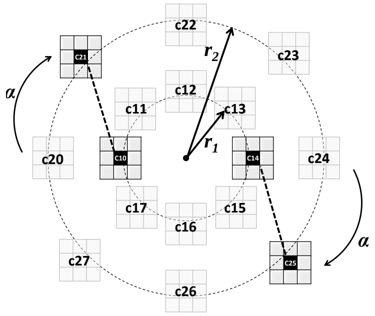

(a)

$$\begin{aligned}&\texttt{FPLBP}_{r1,r2,8,3,1}(p) =\\&f(d(C_{10},C_{21})-d(C_{14},C_{25}))2^0+\\&f(d(C_{11},C_{22})-d(C_{15},C_{26}))2^1+\\&f(d(C_{12},C_{23})-d(C_{16},C_{27}))2^2+\\&f(d(C_{13},C_{24})-d(C_{17},C_{28}))2^3\end{aligned}$$

(b)

(c)

Fig. 3. (a) The Four-Patch LBP code. Four patches involved in computing a single bit value with parameter $\alpha = 1$ are highlighted. (b) The FPLBP code computed with parameters $S = 8$, $w = 3$, and $\alpha = 1$. (c) Code image produced from the image in Fig. 1(b).

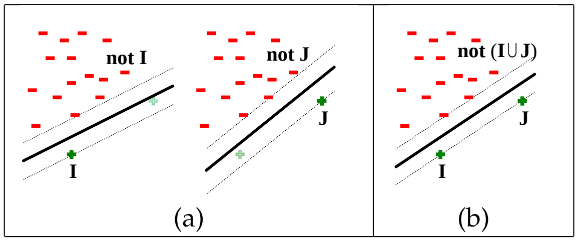

Fig. 4. OSS and TSS scores illustrated. (a) The OSS score is obtained by computing two discriminative models. (b) The Two-Shot score is computed from a single model, taking $\mathbf{I}$ and $\mathbf{J}$ as a positive set, and $\mathbf{A}$ as a negative set. The Two-Shot score reflects the quality of this model.

we train a single discriminative model using both $\mathbf{I}$ and $\mathbf{J}$ as positive examples, and the set $\mathbf{A}$ as a set of negative examples. The Two-Shot score is then defined as a measure of how well this model discriminates the two sets. Again, the particular definition of this score depends on the underlying classifier used. Using the SVM classifier, for example, this can simply be the width of the margin between the two sets. In the following sections we provide detailed analysis of this new similarity score.

4.2 Computing the One-Shot and Two-Shot Similarities

The OSS and TSS scores are actually meta-similarities which can be fitted to work with almost any discriminative learning algorithm. In our experiments, we focused on the Fisher Discriminant Analysis (FDA or LDA) [53], [54] as the underlying classifier. Similarities based on LDA can be efficiently computed by exploiting the fact that the set $\mathbf{A}$ of negative samples is used repeatedly, and that the positive class, which contains just one or two elements, contributes either nothing or a rank-one matrix to the within class covariance matrix.

We focus on binary LDA, which is relevant to this work. Let $p_i \in \mathbb{R}^d, i = 1, 2, ..., m_1$ be a set of positive training examples, and let $n_i \in \mathbb{R}^d, i = 1, 2, ..., m_2$ be a set of negative training examples. Let μ be the average of all points and μ_p (resp. μ_n) be the average of the positive (negative) training set. Two matrices are then considered [55], S_B measuring the covariance of the class centers, and S_W, which is the sum of the covariance matrices of each class. The LDA algorithm computes a projection v which maximizes the quotient:

$$v = \arg\max_v \frac{v^\top S_B v}{v^\top S_W v} \tag{4}$$

In the two class case, v is easily determined as:

$$v = \frac{S_W^+(\mu_p - \mu_n)}{\|S_W^+(\mu_p - \mu_n)\|} \tag{5}$$

Note that we use the pseudo-inverse S_W^+ instead of the inverse S_W^{-1} in order to deal with cases where the within-class covariance matrix is not full rank. This is equivalent to requiring in Eq. 4 that v be spanned by the training vectors.

Once v has been computed, the classification of a new sample $x \in \mathbb{R}^d$ is given by the sign of $v^\top x - v_0$, where v_0 is the bias term. We use the midpoint between the projected means of the classes as the bias value. i.e., in the first stage of the OSS computation, where $\mathbf{I}$ is used as the positive set, and $\mathbf{A}$ as the negative set

$$v_0 = v^\top \frac{I + \mu_A}{2}. \tag{6}$$

This specific choice balances the contribution of the two classes.

LDA-based One-Shot Similarity. By exploiting the fact that the positive set contains a single sample and the negative set is fixed, it can be shown [4] that the LDA-based OSS between samples $\mathbf{I}$ and $\mathbf{J}$, given the auxiliary set $\mathbf{A}$ becomes:

$$\frac{(I-\mu_A)^\top S_W^+(J - \frac{I+\mu_A}{2})}{\|S_W^+(I-\mu_A)\|} + \frac{(J-\mu_A)^\top S_W^+(I - \frac{J+\mu_A}{2})}{\|S_W^+(J-\mu_A)\|} \tag{7}$$

The overall complexity for the OSS per pair is thus $O(d^2)$ once the (pseudo) inverse S_W has been computed. In addition, if similarities are computed for the same point repeatedly, one can factor the positive definite $S_W^+ = HH^\top$ and pre-multiply this point by the factor H.

Free-Scale LDA based One Shot Similarity. The LDA formalization is based on a projection direction given v in Eq. 5. The free-scale LDA is a simplified version in which the projection is done along the unnormalized vector $v = S_W^+(\mu_p - \mu_n)$. The bias term v_0 is computed similarly to LDA (Eq. 6 above).

For binary classification problems, LDA and free-scale LDA (FS-LDA) produce similar results (the sign does not change). However, in the computation of OSS the pre-threshold projection value plays a role, and the similarities based on the two classifiers differ. Specifically, similarities will be larger in magnitude (positive or negative) if $S_W^+(I-\mu_A)$ has a large magnitude, i.e., in cases where I is distant from μ_A in the metric specified by the projection S_W^+. This agrees with the intuition that similarities are more pronounced where the one-sample positive class (I) is well-separated from the negative class (the columns of A).

The OSS based on free-scale LDA is expressed as:

$$(I-\mu_A)^\top S_W^+(J - \frac{I+\mu_A}{2}) + (J-\mu_A)^\top S_W^+(I - \frac{J+\mu_A}{2}) \tag{8}$$

It can be shown that Free-Scale LDA is in fact a conditionally positive definite (CPD) kernel [4]. It can therefore be used directly with translation invariant kernel methods such as SVM and kernel PCA, or give rise to a positive definite kernel (PD) that can be used with any kernel-method.

SVM-based One-Shot Similarity. The computation of OSS based on SVM also benefits from the special structure of the underlying classifications. Consider the hard-margin SVM case. In this case the single positive example becomes a support vector. The maximum margin will be along the line connecting this point and the closest point in set A, which serves as the negative set. Therefore, the two SVM computations per similarity computation are trivial once the points closest to I and J in A are identified. Such simple geometric arguments, which are used in some modern SVM solvers, e.g., [56], fail to work in the soft margin case, and efficient computation for this case is left for future research.

LDA-based Two-Shot Similarity. In the two-shot case, $\mathbf{I}$ and $\mathbf{J}$ serve as the positive class, while the set $\mathbf{A}$ of background samples is used repeatedly as the negative class. In contrast to the One-Shot case, the within class covariance matrix S_W changes from one similarity computation to another.

In order to be robust to the size of the background set and for simplicity, we balance the positive and the negative classes and define the within-class convenience matrix as

$$S_W = \frac{1}{2}S_A + \frac{1}{2}S_{IJ} \tag{9}$$

where $S_A = \frac{1}{|A|}\sum_{x\in A}(x-\mu_A)(x-\mu_A)^\top$, and

$$\begin{aligned} S_{IJ} = \; & \tfrac{1}{2}((I - \tfrac{(I+J)}{2})(I - \tfrac{(I+J)}{2})^\top + \\ & (J - \tfrac{(I+J)}{2})(J - \tfrac{(I+J)}{2})^\top) = \\ & \tfrac{1}{4}(I-J)(I-J)^\top \end{aligned} \tag{10}$$

Since S_{IJ} is a rank-one matrix, the inverse of S_W can be computed by updating the inverse of S_A with accordance to the Sherman-Morrison formula as:

$$\frac{1}{2}S_W^{-1} = S_A^{-1} - \frac{S_A^{-1}(I-J)(I-J)^\top S_A^{-1}}{4 + (I-J)^\top S_A^{-1}(I-J)} \tag{11}$$

If S_W is not full rank, a similar formula can be applied to update the pseudoinverse, based on rank-one updates [57] of the Cholesky factor or SVD of S_A. The details are omitted. Note that the matrix S_W^{-1} need not be computed explicitly. Let $\nu = (I+J)/2 - \mu_A$. From equation 5, v can be computed up to scale as:

$$S_A^{-1}\nu - \frac{S_A^{-1}(I-J)(I-J)^\top(S_A^{-1}\nu)}{4 + (I-J)^\top S_A^{-1}(I-J)}$$

The TSS itself measures the separability of the two classes, i.e., the distance between the centers of the two classes in the direction of v. Thus, once the covariance matrix of the background samples is inverted, computing the TSS requires $O(d^2)$ operations. If points I_i are used repeatedly, $S_A^{-1}I_i$ can be pre-computed, and future TSS computations become $O(d)$.

4.3 The rank based similarity measure

The idea of representing an image by a set of similarities to other images or to prelearned classifiers is well known [58]. Bart and Ullman [59] have proposed to use it for learning a novel class from one example. We have tried using a vector of similarities to the background samples as a face descriptor. Specifically, we generated for image I and for image J vectors of similarities by comparing I or J to each image in A. The resulting vectors produce much worse classification results than the original similarity between I and J.

Instead, we consider a retrieval system in which images I or J are used to retrieve similar images from the set A, and examine the order in which the images are retrieved. In other words, image I (or J) produces an order on the elements of A from the most similar to the least similar.

To compare two such orders, we can employ any one of several non-parametric rank based similarity computation techniques. In such techniques, each image (I or J) is represented by a vector which contains the ranking of each image in the set A from 1 (most similar image) to $|A|$ (least similar image). For example, the correlation between the two rank vectors is one possible similarity between the two permutations.

In our experiments, we have found that it is best to focus on the most similar images. We propose the following rank-sum statistical test. For each of the two samples I and J we compute the rank vectors r_I and r_J described above. Let π_I (π_J) be the order of images in A according to their similarity to I (J). We then compute the similarity s as the sum of the ranking by one image to the first 100 images in the order of the second image:

$$s(I,J) = -\sum_{k=1}^{100} r_I(\pi_J(k)) + r_J(\pi_I(k)). \tag{12}$$

(higher values mean more similar examples). The parameter value of 100 is arbitrary, and provides similar results to other values in the range of 50-150.

4.4 Labeled background samples

The similarity scores introduced in the previous sections do not employ labeling information. They can therefore be applied to a variety of vision problems where collecting unlabeled data is much easier than the collection of labeled data. However, when labeled information is available, these scores do not benefit from it. Here, we focus on the One-Shot Similarity and suggest employing label information by computing OSS scores multiple times. Using the label information we split the background set $\mathbf{A}$ of examples to n sets, $\mathbf{A_i} \subset \mathbf{A}, i = 1..n$, each one containing examples from a single class. The OSS is then computed multiple times, where each time only one subset $\mathbf{A_i}$ is used.

The rational for the split is as follows. The set **A** contains variability due to a multitude of factors including pose, identity and expression. During the computation of the (regular) OSS one tries to judge whether **J** is more likely to belong to the set containing just the point **I** or to the set **A**. **I** contains one person captured at one pose under a particular viewing condition. The classifier trained to distinguish between the two sets can distinguish based on any factor, not necessarily based on the identity of the person.

Now consider the case where the OSS score is applied to a set $\mathbf{A_i}$ which contains a single person, possibly at multiple poses and conditions. In this case the classifier is more likely to distinguish based on identity since all other factors vary within the set $\mathbf{A_i}$. Thus, the score better reflects the desired property of discriminating based on the person in the photograph.

The separation between identity and other factors can be further enhanced by considering OSS scores based on sets which have one of these factors *approximately* constant. For example, if the set $\mathbf{A_i}$ contains people viewed in a certain pose, which is different than the one in **I**, the resulting score would discriminate based on pose. This by itself is not what we seek. However, when combined with other scores to create a multitude of scores, a high pose-based OSS score can indicate that the visual similarity is not necessarily based on identity. Conversely, a low pose-based score indicates that an overall low similarity does not rule out the same label. Note that pose-based OSS scores behave similarly to the regular OSS when **I** and **J** are of a pose similar to the images that are in $\mathbf{A_i}$.

The profile of similarities obtained by the vector of multiple OSS scores is passed during training to a classifier which extracts these relations. Figure 5 demonstrates the various OSS scores for pairs of similar/non-similar identities with similar and non similar poses.

5 Face image pair-matching in the LFW benchmark

We test the effect of the different components introduced in the previous sections on the 10 folds of view 2 of the LFW dataset [5]. In all our tests we use the LFW-a [2], [3] version of the images in the LFW data set[2]. These images were produced by aligning all the original LFW images using the commercial alignment system of face.com.

We begin by describing tests performed with the "image-restricted training" benchmark. This benchmark consists of $6,000$ pairs, half marked "same" and half not, and is divided into 10 equally sized sets. The benchmark test is repeated 10 times, each time using one set for testing and nine others for training. The goal is to

[2] Images available from http://www.openu.ac.il/home/hassner/data/lfwa/

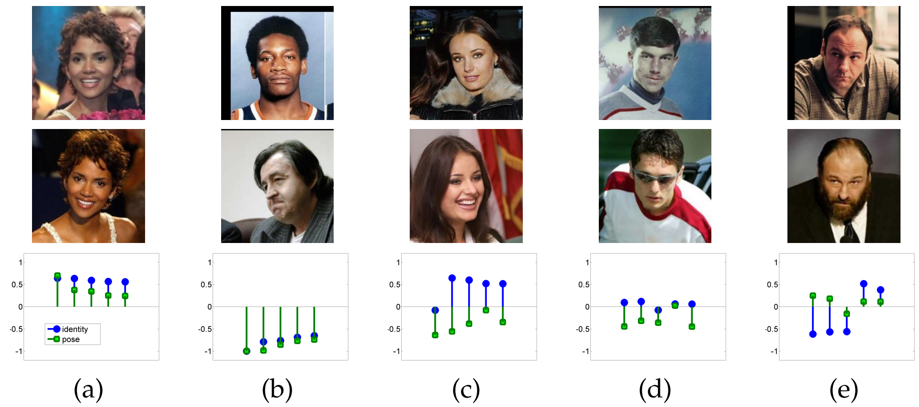

Fig. 5. Each group contains two images and 10 sample multiple OSS scores. Identity based multiple OSS scores are plotted with circle markers and pose based are with squares. As can be seen the value of each type of OSS score is a good indication of the type of similarity between the images of the pair. (a) Same person, same pose. (b) Different persons and pose. (c) Same person, different pose. (d) Different persons, same pose. (e) Same person and pose, however, a mode of variability not modeled in the system is present.

predict which of the test pairs match using only the training data. Other than "same"/"not-same" labels, no information is provided on the identity of the subjects and so labeled background data is unavailable.

We used one of the nine training splits for the background set A and the other eight for classifier training. The background split contains 1,200 images. The subjects in these images do not appear in the test set, as the LFW benchmark is constructed to have subjects in the different splits mutually exclusive [5].

5.1 Pair-matching without background information

Our pair-matching results on the original LFW images, the LFW images aligned using the "Funneling" technique of [15] and the LFWa images are described in Table 2. We use the following image descriptors: the LBP descriptor [24], the Three-patch and Four-patch LBP (TPLBP and FPLBP) descriptors (Section 3), the C1 image descriptor [60], and SIFT [52]. The parameters used in our tests are detailed in Appendix A. Compared to the LBP variants, the SIFT descriptor is less sensitive to misalignment, however, it is easily misled by sharp edges caused by glasses or illumination.

We use either the descriptor vectors or their square roots (i.e., the Hellinger distance). In the latter case, instead of using the descriptor vector $g(I)$ we use $\sqrt{g(I)}$. The 10 descriptor/mode scores in the table are obtained by training a linear SVM on $4,800$ (8 sets) 1D vectors containing the similarity scores. The "Combined" classification is based on learning and classifying the 8D/10D vectors which are the concatenations of the eight/ten 1D vectors (including or excluding SIFT). Such a combination of the output of multiple classifiers is referred to in the literature as stacking [61].

The results are reported in Table 1. The contributions of combining different descriptors and of performing a proper alignment are clearly seen. Note in particular the FPLBP descriptor which performs at about the same quality as the other descriptors, but is far smaller, requiring only 16 bins per histogram (compared to 59 for LBP and 128 for SIFT).

5.2 The contribution of one-shot

Next, we examine the performance of the one-shot measure in Table 2. The descriptors used are the same as above. Here again we use either the original descriptor vectors, or their square roots. The "Combined" classification is based on learning and classifying the 8D/10D vectors which are the concatenations of the eight/ten 1D One-Shot similarities. Results are reported without SIFT (to allow comparison to [1]) and with SIFT. The "Hybrid" results contain all direct (Euclidean) similarities above and the One-Shot similarities. Note the gap in performance compared to the funneled, no-SIFT hybrid previously reported.

Fig. 6 further visualizes the performance of the OSS as a distance function and its contribution to pair-matching classification of LFW images. We compare the OSS measure to the standard Euclidean norm between vectors. We randomly picked five individuals from the LFW set having at least five images each, and five images from each individual. Dissimilarities between all 300 pairs of LBP encoded images were then computed using both the Euclidean norm and OSS scores. The negative training set $\mathbf{A}$ for the OSS scores consisted of $1,000$ images selected at random from individuals having just one image each. The images were then positioned on the plane by computing the 2D Multidimensional-Scaling of these distances (MATLAB's `mdscale` function).

The LFW data set is considered challenging due to its unconstrained nature. Not surprising, no method achieved perfect separation. However, both OSS scores appear to perform better at discriminating between individuals than the L_2 similarity.

TABLE 1
Mean (± standard error) scores on the LFW, Image-Restricted Training benchmark ("view 2") using Euclidean similarities. Please see text for more details.

	Original images		Funneled		Alignment	
Image Descriptor	Euclidian	SQRT	Euclidian	SQRT	Euclidian	SQRT
LBP	0.6649	0.6616	0.6767	0.6782	0.6824	0.6790
Gabor (C1)	0.6665	0.6654	0.6293	0.6287	0.6849	0.6841
TPLBP	0.6713	0.6678	0.6875	0.6890	0.6926	0.6897
FPLBP	0.6627	0.6572	0.6865	0.6820	0.6818	0.6746
Above combined	0.7107 ± 0.0045		0.7062 ± 0.0046		0.7450 ± 0.0068	
SIFT	0.6617	0.6672	0.6795	0.6870	0.6912	0.6986
All combined	0.7223 ± 0.0092		0.7193 ± 0.0049		0.7521 ± 0.0055	

TABLE 2
Mean (± standard error) scores on the LFW, Image-Restricted Training benchmark ("view 2") using OSS. Please see text for more details.

	Original images		Funneled		Alignment	
Image Descriptor	OSS	OSS SQRT	OSS	OSS SQRT	OSS	OSS SQRT
LBP	0.7292	0.7390	0.7343	0.7463	0.7663	0.7820
Gabor (C1)	0.7066	0.7097	0.7112	0.7157	0.7396	0.7437
TPLBP	0.7099	0.7164	0.7163	0.7226	0.7453	0.7514
FPLBP	0.7092	0.7112	0.7175	0.7145	0.7466	0.7436
Above OSS Comb.	0.7582± 0.0067		0.7653 ± 0.0054		0.8002 ± 0.0018	
Above Hybrid	0.7752 ± 0.0063		0.7847 ± 0.0051		0.8255 ± 0.0031	
SIFT	0.7126	0.7199	0.7202	0.7257	0.7576	0.7597
All OSS Combined	0.7673 ± 0.0039		0.7779 ± 0.0072		0.8207 ± 0.0041	
All Hybrid	0.7782 ± 0.0036		0.7895 ± 0.0053		0.8398 ± 0.0035	

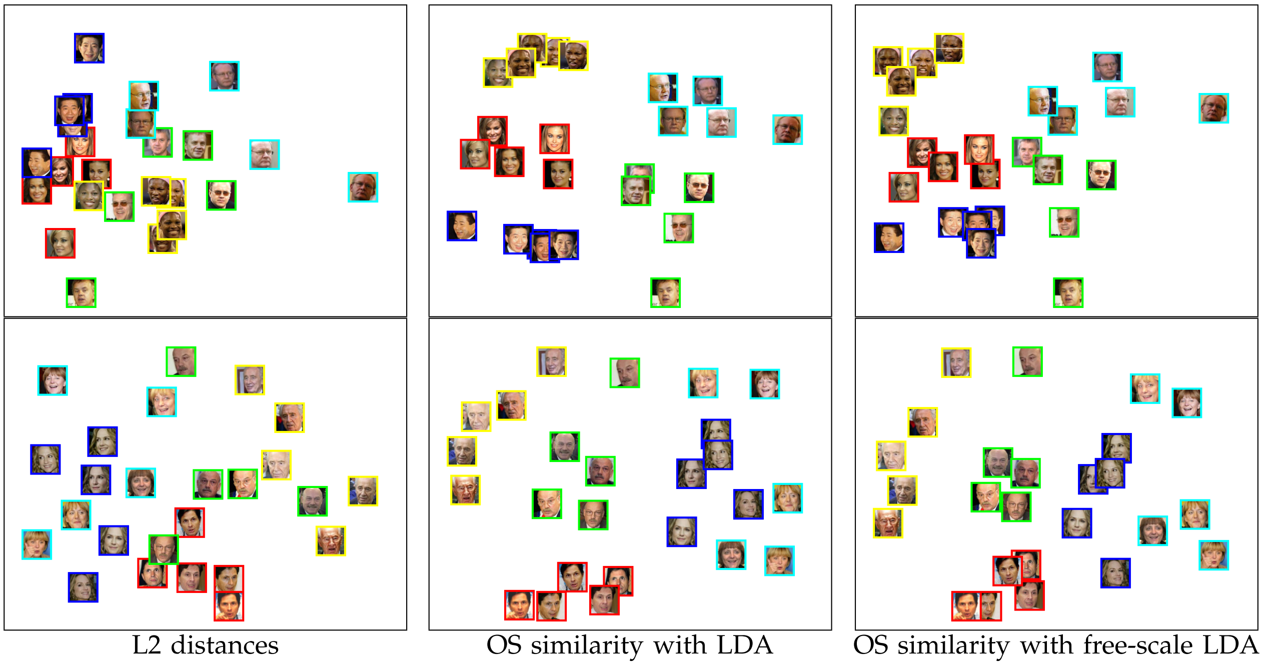

Fig. 6. Visualizing Euclidean distance vs. OSS scores for LFW images. Images positioned according to pairwise Euclidean distances (left), OSS with LDA scores (middle), and OSS with free-scale LDA scores (right). Color frames encode subject IDs.

5.3 The contribution of two-shot

The two-shot similarity adds another layer of information to the OSS. By itself, it is not very discriminative. For the aligned images, all 10 (5 descriptors and using or not using square root) two-shot similarities provide a combined score of 0.6593 ± 0.0076, which is lower than the corresponding figure of 0.8207 for the One-Shot Similarities and the 0.7521 for the baseline similarities.

However, by adding TSS scores to the baseline similarities and the One-Shot Similarities, forming a single similarity vector, the Two-Shot Similarities boost performance considerably. Adding those similarities to the mix increases the performance in the aligned images from 0.8398 ± 0.0035 to 0.8513 ± 0.0037.

5.4 The contribution of the ranking descriptor

The ranking based similarities obtained by the proposed score, which considers the ranking by one example of the first 100 images closest to the other example. It is slightly more effective than Two-Shot Similarity above, and the score obtained by combining all 10 rank similarities using SVM is 0.6918 ± 0.0062. As mentioned in Sec. 4.3, using other forms of representation by similarity are not better.

Similar to the the Two-Shot Similarity above, we examine the contribution of the ranking descriptor when added to the other descriptors. A hybrid descriptor which contains 10 original distances, 10 One-Shot distances, 10 Two-Shot distances, and 10 ranking based distances produces a result of 0.8557 ± 0.0048.

5.5 Combining background similarities beyond LDA

The One-Shot and Two-Shot similarities are frameworks that can be applied with LDA as above or with other classifiers (Section 4.2). Applying it with SVM instead of LDA gives very similar results. However, a considerable boost in performance is obtained when adding SVM based OSS and TSS to those of LDA. Adding those 20 additional dimensions (10 OSS scores and 10 TSS scores using SVM as the underlying classifier) results in a performance of 0.8297 ± 0.0037 for the funneled images and 0.8683 ± 0.0034 for the aligned images, which is currently the state-of-the-art result for the LFW "restricted" protocol.

The ROC curves of the final combined result compared to other published results are presented in Figure 7. The increased performance in comparison to other contributions is apparent in the low-false-positive region, which is the crucial region for most applications.

5.6 The contribution of labeled background samples

The "Unrestricted" test protocol allows training algorithms access to the subject identities in the LFW data set. We use this information by computing multiple OSS scores (Section 4.4) by considering different negative training sets $\mathbf{A_i}$. Each such set contains different images of a single subject, or different subjects viewed from a single pose.

To produce the negative set partitions based on subject identity, we use the unrestricted protocol to retrieve subject labels, and obtain 20 subjects having at least ten images each.

We improve the robustness of our system to pose changes by adding additional OSS scores computed with example sets representing different poses. We produce these sets automatically as follows. We use the coordinates of the seven fiducial points used for aligning the LFW images and producing the LFWa data set. In the creation of LFWa, these coordinates were best fit to a set of predefined "average" coordinates via a similarity transform. Since a similarity transform only accounts for rotation and scale, faces of different poses (and shapes) differ in the aligned coordinates of the fiducial points. We project the 14 dimensional coordinate vectors onto a one-dimensional line using standard PCA on the training set. This line is then partitioned into 10 bins of equal number of images. Each bin then represents a single pose. Figure 8(a) shows an example set of images, all clustered together as having the same pose. Figure 8(b) presents a single representative from each pose set, demonstrating the different pose sets automatically produced by this simple approach.

The vectors of similarity values produced by computing multiple OSS scores are then fed to a linear binary Support Vector Machine classifier, previously trained on similar training vectors. The value output by the classifier is our final classification result.

An additional means of utilizing label information for classification problems is by using techniques for supervised learning of similarity or distance functions, e.g., [36], [62]. We use the ITML code made available by the authors at [62], setting the regularization term to the default value of 0.2, and choosing the lower and upper thresholds to be the default lower and upper tenth percentile. Table 3 presents results with and without ITML, as well as demonstrated the contributions of identity and pose based OSS scores.

One can see that OSS and ITML by themselves improve results considerably. We note that OSS, although unsupervised, provides a large portion of the benefit obtained from ITML. Moreover, the contributions of OSS and ITML accumulate. We also note that Multiple OSS of either type is not better than OSS on the original feature vectors, however, they provide a considerable boost after applying ITML. We attribute this to the fact that applying OSS with small sets of extra negatives ("A_i") is less effective when the underlying metric is not very good. The best results reported in the table, $.8507 \pm .0058$ are the highest results obtained by a single descriptor method.

Finally, we present the results on the LFW benchmark compared to other contributions in Figure 9. Note that unlike all other methods, excluding the LDML-MkNN [19], we use the unrestricted protocol. We present results for our best method (using default parameters), the one based on the square root of the LBP descriptor (0.8517 ± 0.0061 S_E). Also, we further combined 16 Multiple OSS scores, that is 8 descriptors (SIFT, LBP, TPLBP, and FPLBP, as well as all four with square root applied) each trained separately using the ITML + Multiple OSS ID method and the same 8 but with the pose-based multiple shots, into one vector of $16D$. This vector was then classified using a linear SVM classifier (as in the Hybrid

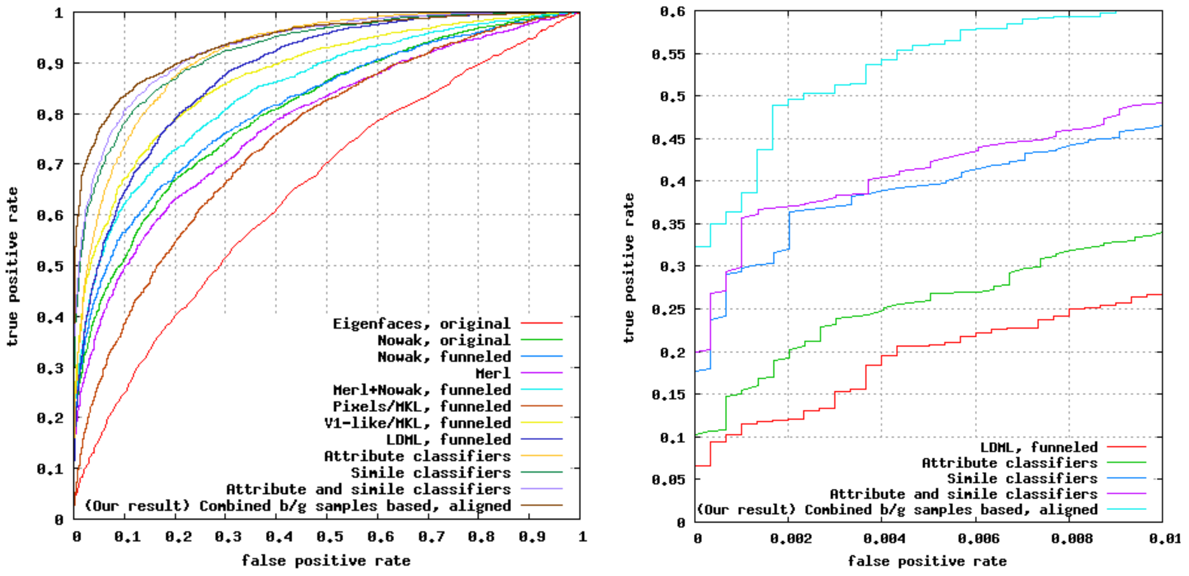

(a) (b)

Fig. 7. ROC curves for View 2 of the LFW data set, “restricted settings”. Each point on the curve represents the average over the 10 folds of (false positive rate, true positive rate) for a fixed threshold. (a) Full ROC curve. (b) A zoom-in onto the low false positive region. The proposed method is compared to scores currently reported in http://vis-www.cs.umass.edu/lfw/results.html

of [1]). The result we obtained for this combination was 0.8950 ± 0.0051 S_E, which is the best result reported so far on the LFW benchmark.

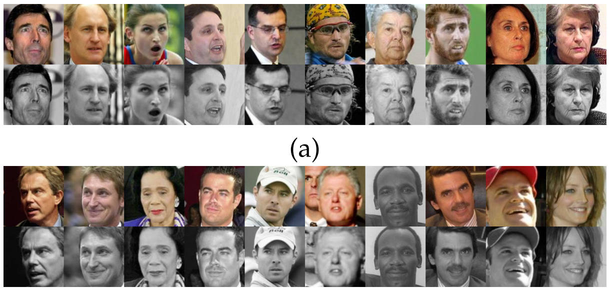

(a)

(b)

Fig. 8. Partitioning into pose. (a) Images in the same pose bin. (b) One example from each pose bin ordered by value. In each subfigure the top row contains the original images and the bottom row contains the aligned versions.

6 Multi-identity face classification in the LFW image set

We next perform multi-person classification tests using the images available in the LFW data set. We use only subjects having enough images to contribute to both “probe” and “gallery” sets. Taking two images per person as probes and two as gallery, we thus employ a subset of the LFW image set consisting of the 610 subjects having at least four images. This subset contains a total of 6733 images. We use a 1-vs-all linear SVM classifier. We use each subject’s gallery images as positive class examples. For the negative set **A** we take 1,000 images selected at random from individuals having only one image.

As previously mentioned, OSS using Free-Scale LDA (FS-LDA) is a conditionally positive definite kernel. It can therefore be used directly in any kernel methods such as SVM. Here, we compare the performance of a 1-vs-all linear SVM classifier (with 1,000 extra negative examples), to that of 1-vs-all SVM with an OSS kernel and LDA as the underlying OSS classifier. We compare the performance of the two methods as a function of the number of subjects N, testing 5, 10, 20, and 50 subject identities. We perform 20 repetitions per experiment. In each, we select N random subjects and choose two random gallery images and a disjoint set of two random probes from each. The results reported in Table 4 indicate that using OSS as the basis of a kernel matrix outperforms the use of the extra negative examples as part of the negative training in a 1-vs-all multi-class classification scheme, as was originally done in [1].

The particular details of the methods compared are:
1-vs-all multi-class SVM. We train one SVM classifier per-subject using only gallery images for training: Each classifier is trained using the gallery images of one class as positive examples and the remaining images as negative examples. A class label is selected based on the highest classification score obtained by any of these classifiers. Linear, Gaussian, and χ^2 SVM kernels are reported. The margin parameter (“C”), and the kernel parameter were searched over a wide range using cross validation on the training set.

1-vs-all SVM with additional negative examples. We

TABLE 3
Mean (± standard error) scores on the LFW, Unrestricted Training benchmark ("view 2") using OSS. Training data now include label information. Please see text for more details.

Image Descriptor	SIFT		LBP		TPLBP	FPLBP
→ version		SQRT		SQRT		
Euclidean distance	.7023±.0067	.7082±.0068	.6795±.0072	.7085±.0076	.6893	.6835
OSS	.7708±.0048	.7817±.0058	.7670± .0051	.7917± .0042	.7598	.7120
MultOSS ID	.7701±.0032	.7831±.0012	.7623± .0072	.7963± .0022	.7602	.7192
MultOSS pose	.7672±.0133	.7773±.0009	.7614± .0023	.7883 ±.0061	.7581	.7122
MultOSS ID + pose	.7741±.0012	.7891±.0021	.7723±.0012	.8001±.0032	.7682	.7222
ITML	.7960±.0097	.8063± .0077	.7665± .0030	.8167± .0054	.7793	.7223
ITML + OSS	.7990± .0063	.8113± .0070	.7867± .0050	.8175± .0055	.7803	.7160
ITML + MultOSS ID	.8320± .0077	.8397±.0070	.8173 ±.0051	.8517± .0061	.8055	.7465
ITML + MultOSS pose	.8153± .0081	.8238± .0082	.7998± .0054	.8340± .0071	.7828	.7325
ITML + MultOSS ID + pose	.8348± .0070	.8397± .0070	.8173± .0054	.8507± .0058	.8075	.7557

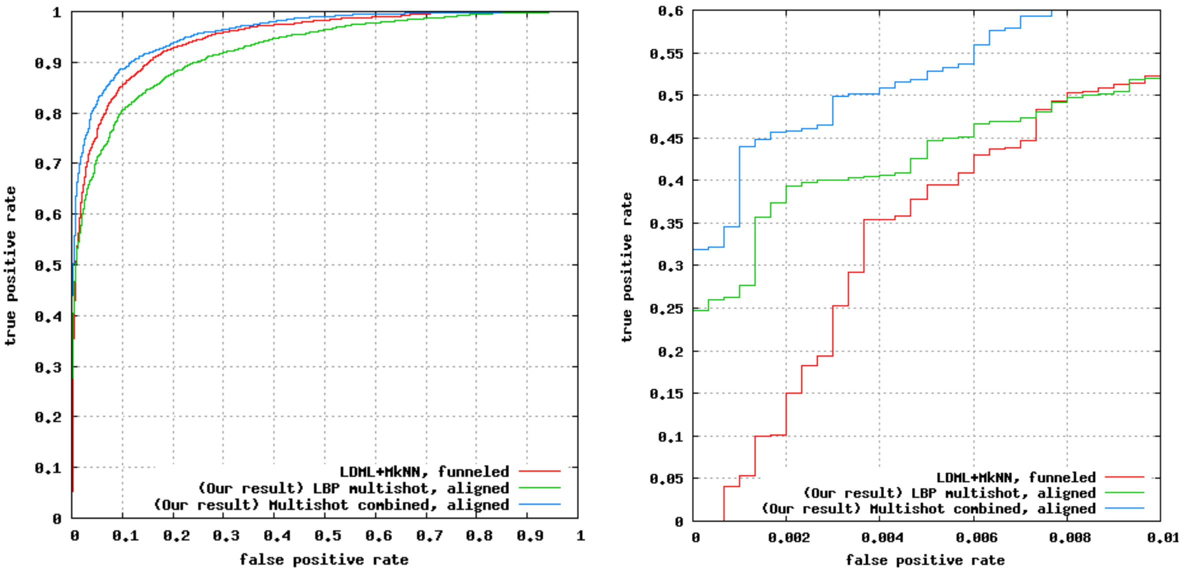

(a) (b)

Fig. 9. ROC curves for View 2 of the LFW data set, using labeled training data through the "unrestricted settings". Each point on the curve represents the average over the 10 folds of (false positive rate, true positive rate) for a fixed threshold. (a) Full ROC curve. (b) A zoom-in onto the low false positive region. The proposed method is compared to scores currently reported in http://vis-www.cs.umass.edu/lfw/results.html

add to the training of each SVM classifier an additional negative examples set **A**, which contains, as mentioned above, $1,000$ images of $1,000$ individuals.

LDA followed by 1-vs-all SVM. The set A was used to compute the projection directions of multiclass LDA. Then, linear SVM was used as a classifier. Note that variants where LDA is followed by Guassian SVM, Nearest Neighbor, or by assigning to the nearest class center performed far worse in our experiments.

1-vs-all SVM with OSS kernel. We use LDA or free-scale LDA as the OSS classifier and the same set **A**. We then employ either the resulting similarities as the kernel function, or the kernel function which is the exponent of $1/50$ times the OSS score. Hence, we have four kernel functions which are then used as the kernel of a 1-vs-all multi-class SVM.

7 Classification beyond LFW

7.1 multi-PIE face recognition tests

We perform multi-person classification tests using the images available in the recently published multi-PIE image set [13], [63]. The images of this set were obtained under controlled laboratory settings and thus allow us to test the robustness of our descriptors and similarity measures to particular sources of variation. Here we focus on the task of recognizing subjects over time.

Of the 337 subjects included in the image set, we select those which attended all four recording sessions over the course of six months. For this set of 126 people, we repeat the test described in [13]. Specifically, the fourth recording session contains two natural expression images for each subject. One was taken as gallery, the other, along with the natural expression images from sessions 1, 2, and 3, were taken as probes. For the

TABLE 4
Classification performance and SE for the person identification experiments. Columns represent the number of subjects (classes). Please see text for more details.

Method	5	10	20	50
Nearest Neighbor	0.5750 ± 0.1333	0.4300 ± 0.0979	0.4913 ± 0.0808	0.3430 ± 0.0405
1-vs-all Linear SVM	0.5500 ± 0.1147	0.4875 ± 0.1099	0.5462 ± 0.0808	0.4005 ± 0.0426
1-vs-all Gaussian SVM	0.5950 ± 0.1099	0.5200 ± 0.1174	0.5037 ± 0.0694	0.3410 ± 0.0509
1-vs-all χ^2 SVM	0.6100 ± 0.1119	0.5250 ± 0.0939	0.5737 ± 0.0845	0.4585 ± 0.0522
1-vs-all SVM with extra neg. examples	0.8050 ± 0.1050	0.7175 ± 0.0783	0.5938 ± 0.0980	0.4520 ± 0.0473
LDA followed by 1-vs-all SVM	0.6050 ± 0.1146	0.5750 ± 0.1118	0.6150 ± 0.0916	0.4925 ± 0.0518
1-vs-all SVM with LDA OSS kernel	0.7850 ± 0.1268	0.7300 ± 0.0785	0.7063 ± 0.0802	0.5865 ± 0.0431
1-vs-all SVM with free-scale LDA OSS kernel	0.7550 ± 0.1432	0.7300 ± 0.0768	0.7000 ± 0.0782	0.5855 ± 0.0365
1-vs-all SVM with exp LDA OSS kernel	0.8150 ± 0.1226	0.7225 ± 0.0716	0.6900 ± 0.0758	0.5790 ± 0.0412
1-vs-all SVM with exp FS LDA OSS kernel	0.8250 ± 0.1164	0.7225 ± 0.0716	0.6863 ± 0.0737	0.5800 ± 0.0450

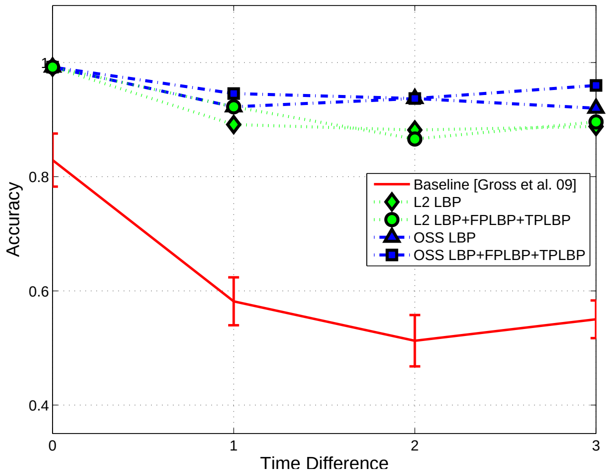

Fig. 10. Performance for Multi-PIE across recording sessions. We compare our results using L2 and OSS scores as similarity measures and a Nearest-Neighbor classifier, to the baseline reported in [13]. Our scores are reported without error bars as we used all available images for testing and did not perform training. It was therefor unnecessary to run multiple tests.

background set A we take one image from each subject participating in session four, but missing at least one of the other sessions (and so not included in the probe and gallery sets). There are 108 such images.

Classification was performed by a simple Nearest Neighbor classifier using either the L2 norm or the OSS scores as measures for similarity. No training was required (other than pre-processing of the negative set A) and therefore only a single test was performed per session. Our results are reported in Figure 10.

The images used for these tests are very typical to controlled Biometrics systems, where subjects corporate with the imaging system, and other sources of variability, such as lighting, are eliminated. Our results in these tests are near perfect. In fact, some of the mistakes made are due to mislabeling of subjects in the database itself. We feel this testifies to the substantial gap between the difficulty of controlled face recognition and face recognition from images taken "in the wild".

7.2 Insect classification

We next test the performance of the OSS as an SVM kernel for multi-label, non-face, image classification. Our goal here is to identify the species of an insect appearing in an image. We used the Moorea Biocode insect image collection [64] containing $6,162$ images and available from the CalPhotos project website [65] (See Fig. 11).

In our tests we use standard Bags-of-Features (BoF) to represent the images [66]. We used the Hessian-Affine extractor and the SIFT [52] descriptor code made available by [67] to produce descriptors. Descriptors were then assigned to clusters to form the BoF representations using the 20k clusters learned from the Flickr60k image set [67].

We tested classification rates with 5, 10, and 50 insect classes selected at random from those having at least four images. Two image descriptors were selected from each class as probe and two as gallery images. The set A was constructed from 2,778 insect images where the specific species in unmarked, and 107 images belonging to classes with fewer than four images.

We compare the performance of the same classifiers used for face recognition in Section 6 with the addition of RCA followed by 1-vs-all SVM: RCA [34] is trained on $\mathbf{A}$ and applied to the data prior to classification. The reported results are the best obtained over a large range of dimensionality reduction parameter tried out ("r"). Here, and in the next item ("LDA then SVM") below, the grouping to classes was done based on the image label which contains either the biological order, family or species.

Our results are reported in Table 5. It can be seen that SVM classifiers with OSS kernels outperformed other classifiers. This is especially true when using the exponential forms. These tests also imply that although OSS with the LDA classifier is not strictly conditionally positive definite [4], it can still be used as a kernel for SVM classification. Additional experiments (not shown) demonstrate that performance seems stable for a wide range of exponent values for the OSS, with no change

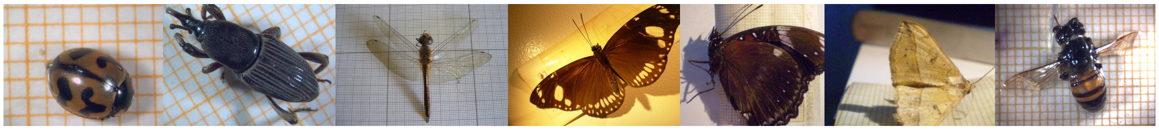

Fig. 11. Examples of insect images from the Moorea Biocode collection [64], [65].

in performance observed for values between 10^{-1} and 10^{-4}.

A note regarding statistical significance. Each experiment in this paper was repeated with the same training and testing split among all training examples. While the variance is sometimes high due to the nature of the datasets, all experiments showing improved results of OSS kernels compared to other method were tested using paired t-tests and shown to be significant at $p < 10^{-5}$.

8 Conclusions

In this work we touch on several key research questions for face identification and general object recognition.

Representing images as vectors: The descriptor based approach to face recognition represents each face image as a vector of descriptors that is independent of other images. There are several alternatives that provide accurate recognition results. For example, the visual similarity method of Nowak and Jurie [47], although not constructed specifically for face recognition, provides a performance baseline on the LFW benchmark that is not trivial to improve upon. With further advancement such methods could prove extremely potent in replacing or complementing descriptor based approaches; However, the scalability of such methods in currently limited due to inherent efficiency constraints.

Role of new descriptors: Face recognition, similar to other domains, e.g., OCR, has been known to benefit from the combination of multiple sources of information. Such information sources may include analysis of facial skin texture, shape of various shape parts, ratios of distances in the face, facial symmetry or lack thereof, etc. Here we show that combining several descriptors, from the same LBP family boosts performance. This suggests that even though the development of new descriptors is an experimental science, which is guided by best practices more than by solid theory, there is room for the introduction of new face encoding methods.

Benchmark practices: The same/not-same benchmarks are convenient in that they provide a binary interface to multiple class problems. Since most real-world vision problems are multi-class in application as well as by nature, the suitability of such benchmarks as a key research tool is not obvious. Put differently, the applicability of the LFW benchmark to real-world face identification problems is not obvious, since a typical vision system is to name a given image, and not to tell for two images whether they are of the same person. It is therefore reassuring that we can see the same pattern of performance and that the same ranking methods in the same-not-same experiments as we observe in the multiple class identification experiments. See also [1].

Background samples: The same/not-same benchmark requires a new class of metric learning techniques since it does not provide information that is suitable for most supervised or semi-supervised methods. These constrains have led us toward the development of a new family of metric learning techniques. These techniques are built around classifiers, and perform one or more training steps per similarity computation. Therefore, the experience gained in supervised learning can be utilized for the task of metric learning. Interestingly, these "n-shot" techniques are able to improve results even in the fully supervised settings, following the application of the most advanced metric learning techniques. Lastly, we note that relying on unlabeled images form other classes, while learning similarities that are tailored to the current sample, is an advancement toward the goal of building ecological vision systems, that learn from an incoming stream of images, and not from large training collections. Such systems might be required to make inferences on novel stimulus based on past stimulus belonging to previously encountered classes.

References

[1] L. Wolf, T. Hassner, and Y. Taigman, "Descriptor based methods in the wild," in *Faces in Real-Life Images Workshop in European Conference on Computer Vision (ECCV)*, 2008.

[2] Y. Taigman, L. Wolf, and T. Hassner, "Multiple one-shots for utilizing class label information," in *The British Machine Vision Conference (BMVC)*, Sept. 2009.

[3] L. Wolf, T. Hassner, and Y. Taigman, "Similarity scores based on background samples," in *Asian Conference on Computer Vision (ACCV)*, Sept. 2009.

[4] ——, "The one-shot similarity kernel," in *IEEE International Conference on Computer Vision (ICCV)*, Sept. 2009.

[5] G. B. Huang, M. Ramesh, T. Berg, and E. Learned-Miller, "Labeled faces in the wild: A database for studying face recognition in unconstrained environments," University of Massachusetts, Amherst, Technical Report 07-49, October 2007.

[6] N. Kumar, A. Berg, P. Belhumeur, and S. Nayar, "Attribute and simile classifiers for face verification," in *International Conference on Computer Vision (ICCV)*, 2009. [Online]. Available: www.cs.columbia.edu/CAVE/databases/pubfig

[7] "LFW benchmark results," Website, http://vis-www.cs.umass.edu/lfw/results.html.

[8] P. Phillips, H. Moon, P. Rauss, and S. Rizvi, "The FERET evaluation methodology for face recognition algorithms," *IEEE Transactions on Pattern Analysis and Machine Intelligence (TPAMI)*, vol. 22, no. 10, 2000.

[9] P. Phillips, P. Flynn, T. Scruggs, K. Bowyer, J. Chang, K. Hoffman, J. Marques, J. Min, and W. Worek, "Overview of the face recognition grand challenge," in *IEEE Computer Vision and Pattern Recognition (CVPR)*, 2005, pp. 947–954.

[10] P. Phillips, P. Flynn, W. Scruggs, K. Bowyer, and W. Worek, "Preliminary face recognition grand challenge results," in *International Conference on Automatic Face and Gesture Recognition*, 2006, pp. 15–24.

TABLE 5
Classification performance and standard errors for the insect identification experiments. Each experiment was repeated 100 times, and the average recognition rate and the standard deviation of the rate are reported. Columns represent the number of insect classes.

Method	5	10	50
Nearest Neighbor	0.2750 ± 0.1372	0.1725 ± 0.0550	0.0530 ± 0.0258
1-vs-all Linear SVM	0.3300 ± 0.1418	0.2500 ± 0.0918	0.1140 ± 0.0272
1-vs-all Gaussian SVM	0.2800 ± 0.1473	0.1875 ± 0.0510	0.0680 ± 0.0226
1-vs-all χ^2 SVM	0.3600 ± 0.1635	0.2575 ± 0.1017	0.1025 ± 0.0281
1-vs-all SVM with extra neg. examples	0.4100 ± 0.1629	0.2625 ± 0.1398	0.1270 ± 0.0266
RCA followed by 1-vs-all SVM	0.3850 ± 0.1538	0.3000 ± 0.1046	0.1335 ± 0.0283
LDA followed by 1-vs-all SVM	0.3800 ± 0.1795	0.2300 ± 0.1069	0.0945 ± 0.0221
1-vs-all SVM with LDA OSS kernel	0.3900 ± 0.1447	0.2875 ± 0.1134	0.1285 ± 0.0281
1-vs-all SVM with free-scale LDA OSS kernel	0.3250 ± 0.1209	0.2425 ± 0.0963	0.1110 ± 0.0261
1-vs-all SVM with exponential LDA OSS kernel	0.4300 ± 0.1559	0.3075 ± 0.1398	0.1430 ± 0.0301
1-vs-all SVM with exponential free-scale LDA OSS kernel	0.4400 ± 0.1501	0.3200 ± 0.1271	0.1380 ± 0.0302

[11] P. Phillips, W. Scruggs, A. OToole, P. Flynn, K. Bowyer, C. Schott, and M. Sharpe, “FRVT 2006 and ICE 2006 large-scale results,” in *NISTIR 7408*, 2007.

[12] T. Sim, S. Baker, and M. Bsat, “The cmu pose, illumination, and expression database,” *IEEE Transactions on Pattern Analysis and Machine Intelligence (TPAMI)*, vol. 25, no. 1, pp. 1615 – 1618, December 2003.

[13] R. Gross, I. Matthews, J. Cohn, T. Kanade, and S. Baker, “Multi-pie,” *Image and Vision Computing*, 2009.

[14] P. Viola and M. Jones, “Robust real-time face detection,” *International Journal of Computer Vision (IJCV)*, vol. 57, no. 2, pp. 137–154, 2004.

[15] G. Huang, V. Jain, and E. Learned-Miller, “Unsupervised joint alignment of complex images,” in *IEEE International Conference on Computer Vision*, 2007.

[16] G. B. Huang, M. J. Jones, and E. Learned-Miller, “LFW results using a combined nowak plus MERL recognizer.” in *Faces in Real-Life Images Workshop in European Conference on Computer Vision (ECCV)*, 2008.

[17] C. Sanderson and B. Lovell, “Multi-region probabilistic histograms for robust and scalable identity inference,” in *International Conference on Biometrics (ICB)*, 2009.

[18] N. Pinto, J. DiCarlo, and D. Cox, “How far can you get with a modern face recognition test set using only simple features?” in *Computer Vision and Pattern Recognition (CVPR)*, 2009.

[19] M. Guillaumin, J. Verbeek, C. Schmid, I. Lear, and L. Kuntzmann, “Is that you? Metric learning approaches for face identification,” in *International Conference on Computer Vision (ICCV)*, 2009.

[20] R. Brunelli and T. Poggio, “Face recognition: Features versus templates,” *IEEE Transactions on Pattern Analysis and Machine Intelligence*, vol. 15, no. 10, pp. 1042–1052, 1993.

[21] L. Wiskott, J.-M. Fellous, N. Krüger, and C. von der Malsburg, “Face recognition by elastic bunch graph matching,” *PAMI*, vol. 19, no. 7, pp. 775–779, 1997.

[22] E. Meyers and L. Wolf, “Using biologically inspired features for face processing,” *Internation Journal of Computer Vision*, vol. 76, no. 1, pp. 93–104, 2008.

[23] X. Tan and B. Triggs, “Fusing gabor and LBP feature sets for kernel-based face recognition,” in *Analysis and Modelling of Faces and Gestures*, ser. LNCS, vol. 4778. Springer, oct 2007, pp. 235–249. [Online]. Available: http://lear.inrialpes.fr/pubs/2007/TT07a

[24] T. Ojala, M. Pietikainen, and D. Harwood, “A comparative-study of texture measures with classification based on feature distributions,” *Pattern Recognition*, vol. 29, no. 1, pp. 51–59, Jan. 1996.

[25] T. Ojala, M. Pietikäinen, and T. Mäenpää, “Multiresolution gray-scale and rotation invariant texture classification with local binary patterns,” *IEEE Trans. Pattern Anal. Mach. Intell.*, vol. 24, no. 7, pp. 971–987, 2002.

[26] T. Ojala, M. Pietikäinen, and T. Mäenpää, “A generalized local binary pattern operator for multiresolution gray scale and rotation invariant texture classification,” in *ICAPR '01: Proceedings of the Second International Conference on Advances in Pattern Recognition*. London, UK: Springer-Verlag, 2001, pp. 397–406.

[27] T. Ahonen, A. Hadid, and M. Pietikainen, “Face description with local binary patterns: Application to face recognition,” *IEEE Transactions on Pattern Analysis and Machine Intelligence*, vol. 28, no. 12, pp. 2037–2041, Dec. 2006.

[28] M. Heikkilä, M. Pietikäinen, and C. Schmid, “Description of interest regions with center-symmetric local binary patterns,” in *Computer Vision, Graphics and Image Processing, 5th Indian Conference*, 2006, pp. 58–69.

[29] L. Zhang, R. Chu, S. Xiang, S. Liao, and S. Li, “Face detection based on multi-block LBP representation,” in *IAPR/IEEE International Conference on Biometrics*, 2007.

[30] S. Belongie, J. Malik, and J. Puzicha, “Shape context: A new descriptor for shape matching and object recognition,” in *Advances in Neural Information Processing Systems 13*, T. K. Leen, T. G. Dietterich, and V. Tresp, Eds. MIT Press, 2001, pp. 831–837.

[31] H. Zhang, A. Berg, M. Maire, and J. Malik, “Svm-knn: Discriminative nearest neighbor classification for visual category recognition,” in *CVPR*, 2006.

[32] M. Bilenko, S. Basu, and R. Mooney, “Integrating constraints and metric learning in semi-supervised clustering,” in *International Conference on Machine Learning (ICML)*, 2004.

[33] N. Cristianini, J. Kandola, A. Elisseeff, and J. Shawe-Taylor, “On kernel-target alignment,” in *The Neural Information Processing Systems (NIPS)*, 2002.

[34] N. Shental, T. Hertz, D. Weinshall, and M. Pavel, “Adjustment learning and relevant component analysis,” in *ECCV*, 2002.

[35] K. Weinberger, J. Blitzer, and L. Saul, “Distance metric learning for large margin nearest neighbor classification,” *The Neural Information Processing Systems (NIPS)*, 2006.

[36] E. Xing, A. Y. Ng, M. Jordan, and S. Russell, “Distance metric learning, with application to clustering with side-information,” in *The Neural Information Processing Systems (NIPS)*, 2003.

[37] L. Fei-Fei, R. Fergus, and P. Perona, “One-shot learning of object categories,” *PAMI*, vol. 28, no. 4, pp. 594–611, 2006.

[38] M. Fink, “Object classification from a single example utilizing class relevance pseudo-metrics,” in *The Neural Information Processing Systems (NIPS)*, 2004.

[39] O. Chapelle, B. Scholkopf, and A. Zien, *Semi-Supervised Learning*. MIT Press, Cambridge, MA, 2006.

[40] T. Joachims, “Transductive learning via spectral graph partitioning,” in *International Conference on Machine Learning (ICML)*, 2003, pp. 290–297.

[41] A. Quattoni, M. Collins, and T. Darrell, “Transfer learning for image classification with sparse prototype representations,” *Computer Vision and Pattern Recognition (CVPR), 2008*, June 2008.

[42] A. Bar-Hillel, T. Hertz, N. Shental, and D. Weinshall, “Learning distance functions using equivalence relations,” in *ICML*, 2003.

[43] W. Liu, S. Hoi, and J. Liu, “Output Regularized Metric Learning with Side Information,” in *Proceedings of the 10th European Conference on Computer Vision (ECCV)*, 2008, pp. 358–371.

[44] G. Chechik and N. Tishby, “Extracting relevant structures with side information,” in *The Neural Information Processing Systems (NIPS)*, 2002, pp. 857–864.

[45] P. Jain, B. Kulis, and K. Grauman, “Fast Image Search for Learned Metrics,” in *IEEE Conference on Computer Vision and Pattern Recognition, 2008. CVPR 2008*, 2008, pp. 1–8.

[46] ——, “Fast similarity search for learned metrics,” in *University of Texas at Austin, Technical Report #TR-07-48*, September 2007.

[47] E. Nowak and F. Jurie, “Learning visual similarity measures for comparing never seen objects,” in *IEEE Conference on Computer Vision and Pattern Recognition*, June 2007.

[48] S. Ullman and E. Sali, “Object classification using a fragment-based representation,” in *the First IEEE International Workshop on Biologically Motivated Computer Vision*. London, UK: Springer-Verlag, 2000, pp. 73–87.

[49] L. Wolf, X. Huang, I. Martin, and D. Metaxas, “Patch-based texture edges and segmentation,” in *European Conference on Computer Vision*, 2006, pp. 481–493.

[50] E. Shechtman and M. Irani, “Matching local self-similarities across images and videos,” *CVPR*, pp. 1–8, June 2007.

[51] X. Tan and B. Triggs, “Enhanced Local Texture Feature Sets for Face Recognition Under Difficult Lighting Conditions,” in *Analysis and modeling of faces and gestures (AMFG)*, 2007.

[52] D. Lowe, “Distinctive image features from scale-invariant keypoints,” *Int. J. Comput. Vision*, vol. 60, no. 2, pp. 91–110, 2004.

[53] R. Fisher, “The use of multiple measurements in taxonomic problems,” *Annals Eugenics*, vol. 7, pp. 179–188, 1936.

[54] T. Hastie, , R. Tibshirani, and J. Friedman, *The elements of statistical learning*. Springer, 2001.

[55] R. O. Duda, P. E. Hart, and D. G. Stork, *Pattern classification, 2nd ed.* Wiley, 2001.

[56] A. Bordes and L. Bottou, “The huller: A simple and efficient online svm,” in *ECML*, 2005.

[57] M. Brand, “Fast low-rank modifications of the thin singular value decomposition,” *Linear Algebra and its Applications*, vol. 415, no. 1, pp. 20 – 30, 2006. [Online]. Available: http://www.sciencedirect.com/science/article/B6V0R-4H6GPWW-2/2/38c4c644be30c47ecac3d19953b89fe9

[58] S. Edelman, *Representation and recognition in vision*. Cambridge, MA, USA: MIT Press, 1999.

[59] E. Bart and S. Ullman, “Single-example learning of novel classes using representation by similarity,” in *British Machine Vision Conference*, 2005.

[60] M. Riesenhuber and T. Poggio, “Hierarchical models of object recognition in cortex,” *Nature Neuroscience*, vol. 2, no. 11, pp. 1019–1025, 1999.

[61] D. H. Wolpert, “Stacked generalization,” *Neural Netw.*, vol. 5, no. 2, pp. 241–259, 1992.

[62] J. Davis, B. Kulis, P. Jain, S. Sra, and I. Dhillon, “Information-theoretic metric learning,” in *International Conference on Machine Learning (ICML)*, June 2007, pp. 209–216.

[63] R. Gross, I. Matthews, J. Cohn, T. Kanade, and S. Baker, “Multi-pie,” in *Proceedings of the Eighth IEEE International Conference on Automatic Face and Gesture Recognition*, 2008.

[64] “Moorea biocode insect photo collection,” Website, http://bscit.berkeley.edu/biocode/.

[65] “Calphotos image collection,” Website, http://calphotos.berkeley.edu/.

[66] J. Sivic and A. Zisserman, “Video google: A text retrieval approach to object matching in videos,” in *ICCV*, 2003.

[67] H. Jegou, M. Douze, and C. Schmid, “Hamming embedding and weak geometry consistency for large scale image search,” in *ECCV*, 2008.

[68] http://www.ee.oulu.fi/mvg/page/lbp_matlab.

APPENDIX A
THE PARAMETERS USED IN OUR EXPERIMENTS

Preprocessing For descriptor based methods, all LFW-funneled images used in our tests were cropped to 110×115 pixels around their center. Following [28] we further applied an adaptive noise-removal filter (Matlab’s `weiner2` function) and normalized the images to saturate 1% of values at the low and high intensities.

Descriptor parameters The parameter tuning, when performed, was done on “view 1” of the LFW dataset, which is intended for such tests. The image descriptors for all LBP variants are constructed by concatenating histograms produced for 35 non-overlapping blocks of up to 23×18 codes. To produce the LBP descriptors we use the MATLAB source code available from [68]. Results are obtained with “uniform” LBP of radius 3 and considering eight samples. The parameters of the patch based LBP descriptors are $r_1 = 2$, $S = 8$, $w = 5$ for TPLBP, and $r_1 = 4$, $r_2 = 5$, $S = 3$, $w = 3$ for FPLBP. To compute a global SIFT descriptor, we subdivide the image into a grid of 7x7, and compute a 128D SIFT descriptor for each one of the 49 patches. All descriptors are then concatenated to a single vector.